

RESEARCH

Open Access



Multiple low-dose radiation ameliorates type-2 diabetes mellitus via gut microbiota modulation to activate TLR4/MyD88/NF- κ B pathway

Lijing Qin^{1†}, Rongrong Liu^{1†}, Zhen Jia^{1,2}, Weiqiang Xu¹, Li Wang¹, Hongyuan Tian¹, Xinru Lian¹, Wen Li¹, Yali Qi³, Huan He^{1*} and Zhicheng Wang^{1*}

Abstract

Background Type 2 diabetes mellitus (T2DM) is the fastest-growing metabolic disease in the world. The gut microbiota is linked to T2DM. Recent studies have showed that the metabolism of gut microbiota can trigger T2DM. Low dose radiation (LDR) has been proved to activate various protective bioeffects on diabetes. However, the underlying mechanisms remain unclear.

Methods In this study, T2DM model was established using high fat diet combined with streptozocin (STZ) injection in C57BL/6 mice, and then exposed to multiple 75 mGy LDR every other day for one month. The changes of blood glucose levels, body weight, and the damage of pancreas were measured. In addition, 16 S rDNA amplicon sequencing was used to detect gut microbiota alteration. Metabolic profiling was carried out using the liquid mass spectrometry system, followed by the combinative analysis of gut microbiota alteration. Furthermore, the inflammatory factors and related pathways were detected.

Results We found that LDR attenuate blood glucose levels and the weights of body in T2DM mice, and reduce pancreas impairment. In addition, in the gut, LDR regulated the relative abundance of Bacilli, Desulfobacterota, Verrucomicrobiota, and Proteobacteria. The non-target metabolomics analysis found that LDR significantly improve the metabolic abnormalities in T2DM, which is closely related to the gut microbiota abundance. Furthermore, the inflammatory effects activated by TLR4/MyD88/NF- κ B pathways in T2DM were ameliorated by LDR.

Conclusion These results suggest that LDR may exert a beneficial role in T2DM by modulating gut microbiota and metabolites, especially in TLR4/MyD88/NF- κ B pathway.

Keywords Type 2 diabetes mellitus, Low dose radiation, Gut microbiota, Metabolites, Toll-like receptor 4

[†]Lijing Qin and Rongrong Liu contributed equally to this work.

*Correspondence:

Huan He

hehuan@jlu.edu.cn

Zhicheng Wang

zhicheng@jlu.edu.cn

Full list of author information is available at the end of the article



Introduction

Diabetes is a common problem facing modern society, type 2 diabetes mellitus (T2DM) accounts for more than 90% of the total number of diabetes patients, which is characterized by insulin resistance, a defect in the ability of insulin to absorb glucose, and patients often have metabolic abnormalities [1–3]. The factors and mechanisms that trigger T2DM have been intensely discussed, genetic factor, high caloric intake, and physical inactivity are the major risk factors [4]. Insulin is produced by the β -cells of pancreas, if the amount of insulin fails to compensate the physical demand, the person will develop hyperglycemia [5]. Poorly controlled diabetes and the metabolic disorders associated with T2DM, such as impaired lipid, amino acids, and bile acids, can modulate insulin sensitivity. The etiologies of metabolic disorders are closely related with obesity resulted from high fat diet (HFD) consumption, energy expenditure, genetics, level of physical activity, etc [6–8]. Therefore, it is very meaningful to further investigate the influencing factors of metabolic dysfunction.

In recent years, the gut microbiota, described as “the second genome of the body”, potentially affect obesity, energy metabolism, glucose metabolism, and immunity [9–11]. Studies have shown that the excessive intake of salt, sugar, and fat will lead to over nutrition, and affect the diversity and stability of intestinal microbes causing chronic inflammation in the intestines and insulin resistance, ultimately lead to diabetes [12–14]. Many inflammatory cytokines, such as tumor necrosis factor- α (TNF- α), interleukin-6 (IL-6), and interferon γ (IFN- γ), have been reported to be elevated in the diabetic models [15]. These cytokines also play a rather important role through a positive feedback loop, primarily in the nuclear factor- κ B (NF- κ B) activation [16]. In gut, the elevation of sugar metabolites will cause pathological increase of bacteria *Enterobacter* and other intestinal flora, resulting in inflammatory response and insulin resistance [17, 18]. In some studies, the relationships between Toll-like receptor 4 (TLR-4) and microbial metabolites, such as LPS, butyrate and folate were described. Additionally, microbial metabolites promote the development of inflammation and insulin resistance through TLRs signaling pathway [19]. Therefore, the interventions targeting microbiota might influence the glucose-lowering effects [20].

Previous studies have shown that low dose radiation (LDR) can activate anti-oxidative and anti-inflammatory effects [21]. LDR also has multiple beneficial effects on renal dysfunction, cardiac inflammation, brain injury, and reproductive damage in diabetes [22–24]. Xiaodan Liu et al. found that BALB/c mice suffered LDR exhibited changes in the composition of gut microbiota through

detecting feces [25]. The changes include increasing the abundance of *Clostridium*, *Helicobacter*, and *Oscilibacter*, while decreasing the abundance of *Bacteroides* and *Barnesiella*. Additionally, several studies on murine and human models showed that HFD increased endotoxemia, which disrupted the epithelial barrier and enhanced permeation of microbial metabolites [18, 26, 27]. Other studies demonstrated a significant increase in the *Desulfovibrionaceae* family in both obese human and mice compared to the lean individuals, which might influence pro-inflammatory through LPS [28, 29].

Over the years, although substantial efforts were made to elucidate the mechanisms of protective effects of LDR on T2DM, it is still unclear. In this study, we investigated whether LDR exhibits protective property in diabetes, and the functions and mechanisms of gut microbiota and metabolites involved in the process.

Materials and methods

T2DM model establishment and LDR exposure

Male wild-type C57BL/6 mice (SPF, 16~22 g, 6~8 weeks) were supplied by Beijing HFK Bioscience CO. LTD. (Beijing, China). The mice bred at the laboratory Animal Center of Public Health School of Jilin University (license No. SYXK (Ji) 2021–0003). The study protocol was approved by the Medical Ethics Committee of Jilin University and was conducted in accordance with the Institutional Guide for the Ethical Use of Animals (2024-07-004). The experiment was started after 1 week of acclimation of mice to laboratory conditions. Eighty mice were randomized into vehicle and T2DM groups, 20 mice in vehicle group were fed by a low-fat diet (LFD, 10% fat) and 60 mice in T2DM group were fed by high-fat diet (HFD, 60% fat) for 16 weeks, respectively. HFD-fed mice were intraperitoneally injected with Streptozotocin (STZ) (for 5 consecutive days, 30 mg/kg body weight; dissolved in 0.1 M citrate buffer, pH 4.5) to induce T2DM [30]. Mouse with random blood glucose levels over 11.1 M measured at 4 days after STZ injection were considered diabetic and select 20 mice that have successfully constructed the diabetes model for subsequent related experiments. Subsequently, the LFD-fed mice were randomly divided into 2 subgroups with 10 mice in each group, including Control (LFD) and LDR (75 mGy+LFD), and diabetic mice were randomly divided into 2 subgroups with 10 mice in each group, including T2DM (HFD) and LDR+T2DM (75 mGy+HFD). For LDR subgroup, mice were exposed to 75 mGy each time (dose rate: 13.4 mGy/min), exposure was performed every other day for 1 month, total dose was 1.05 Gy. The doses and rates were selected based on a report by the United Nations Scientific Committee on Atomic Radiation (UNSAR, 1986) and on previous studies [24].

All mice were kept in a specific pathogen-free environment at room temperature ($24 \pm 1^\circ\text{C}$), relative humidity (25~40%), and a 12 h light/dark cycle. All mice were provided with a corresponding diet and body weight was detected weekly at the end of the experiments. Upon the completion of the experimental procedures, the mice were subjected to anesthesia with a dosage of 100 mg/kg sodium phenobarbital. Open abdominal surgery for fecal extraction, cardiac puncture was performed to collect blood samples. All mice were sacrificed by cervical dislocation. After sacrificing, the small intestine, spleen, and pancreatic islet tissues of mice were excised and meticulously cleaned. Subsequently, the tissues were either fixed with 4% paraformaldehyde (PFA) or preserved by freezing at -80°C , or conduct other experiments immediately.

Reagents and antibodies

STZ were purchased from Sigma-Aldrich (St Louis, MO USA). IL-4 (APC, 17–7041-82) and IL-17 A (APC, 17–7177-81) was obtained from eBioscience (San Diego, CA, USA). MyD88 (BS3521) and TLR4 (BS91353) was obtained from Bioworld (Bloomington, MN, USA). p-NF- κ B-p65 (YT0192), p-p38 (YP0338), Biotin-conjugated goat anti-rabbit IgG (H+L) (RS0002), and Biotin-conjugated goat anti-mouse IgG (H+L) (RS0001) was obtained from Immunoway (Plano, TX, USA). TRIzol RNA isolation reagent was purchased from Invitrogen (Carlsbad, CA, USA). Other chemicals and reagents were analytic grade.

Glucose tolerance test

Food was withheld 16 h before testing; mice (HFD) were administrated with glucose (1.5 mg/g) by intraperitoneal injection with 5% glucose. Blood samples were taken by tail pick at 0, 15, 30, 60, 90 and 120 min after glucose injection, glucose levels were measured using glucometer (Sinocare, Hunan, China).

Histological and immunohistochemical analysis

Pancreatic and intestinal tissues were fixed with 4% PFA for more than 48 h at room temperature and processed for paraffin embedding. Subsequently, 4 μm sections were prepared for hematoxylin and eosin (H&E) and immunohistochemical analysis. Pancreatic sections were stained with H&E to routine histopathological examination and morphometric analysis at 200 magnifications. Immunohistochemistry examination was used to detect TLR4, MyD88, p-NF- κ B-p65 and p-p38 in intestinal tissues, HRP-conjugated secondary antibody was added after primary antibodies incubation, and samples were incubated for 10 min at room temperature. Then, 3, 3'-diamino-benzidine (DAB) color solution was added, and nucleus was stained with hematoxylin for 3 min

before dehydration. Then, the tissue sections were sealed using neutral gum. Under the light microscopy, DAB positive expression was brownish-yellow and the nucleus was blue. Photographs were taken under a microscopy.

16S rDNA sequencing

Mice fecal samples were collected from the Control, LDR, T2MD, and LDR + T2MD group, respectively. The total fecal microbiota DNA was extracted from fecal samples using a QIAamp Fast DNA stool Mini Kit (Qiagen, Cat# 51604) and full length sequence of 16 S rDNA was amplified by polymerase chain reaction (PCR). The denoised sequences were binned into operational taxonomic units (OTUs) with 97% similarity using USEARCH (version 10.0). Taxonomy was assigned to all OTUs by searching against the Silva databases (Release128) using QIIME software. The differences of gut microbiota composition were further analyzed, and the relative abundance curve was used to reflect species diversity and abundance of samples. Alpha-diversity indexes, including ACE and Chaos and Simpson, were performed to comparably analyze the species richness and uniformity. Beta-diversity was used to evaluate the species complexity among different groups. The distribution of gut microbiota at the class level in different groups were compared, and the characteristic strains were researched by Linear discriminant analysis Effect Size (LEfSe), OTUs with relative abundance greater than 0.5% were screened for analysis based on Linear Discriminant Analysis (LDA) score. Correlation analysis were performed using "Spearman" ($|r| \geq 0.1$, $P < 0.05$), and functional prediction were performed using "PICRUST2" R package to analyze the differential component in KEGG pathways in different samples or groups, the differences in functional genes and their effects on metabolic pathways can be assessed.

Untargeted metabolic profiling

An equal volume of serum from mice in each group were used to metabolite extraction. Untargeted metabolomics detection was performed using a Waters ACQUITY UPLC I-Class and Xevo G2-XS QTOF system. Peak extraction and alignment were performed using the Progenesis QI software. Untargeted metabolomics analysis was performed by Principal Component Analysis (PCA), Difference multiple analysis, metabolite annotation, and receiver operating characteristic curve (ROC), etc.

Flow cytometry

Fresh spleen tissues were collected from each group and washed by PBS, the single cell suspension was prepared. The cell concentration was adjusted to 1×10^7 cells/mL, and the cells were washed using 1 mL PBS. After cells were fixed and membranes were broken, 5 μL IL-4 (APC)

and IL-17 A (APC) antibodies were added and mixed according to the manufacturer's protocols. The cells were stained in the dark for 30 min and were washed using PBS. Furthermore, 10,000 cells were collected by BD Flow Cytometry (Franklin Lakes, NJ, USA) and analyzed by FlowJo software.

Quantitative real-time PCR (qRT-PCR)

Total RNA of mice intestine was extracted by TRIzol reagent according the manufacturer's protocols. The concentration of RNA was determined using Bio Tek Epoch (USA) and then cDNA was synthesized using a reverse transcription assay kit (EasyScript® All-in-One First-Strand cDNA Synthesis SuperMix for qPCR, TransGen Biotech). The mRNA expression levels were detected by qRT-PCR using SYBR Green master mix obtained from TransGen Biotech Co. (Beijing, China).

The following primers were synthesized by Kumei Inc. (Jilin, China), GAPDH: 5'-AAATGGTGAAGGTCG GTGTG-3' (F), 5'-TGAAGGGGTCGTTGATGG-3' (R); TLR4: 5'-ATGGCATGGCTTACACCACC-3' (F), 5'-GAGGCCAATTTTGTCTCCACA-3' (R); MyD88: 5'-ATCGCTGTTCTTGAACCCTCG-3' (F), 5'-CTC ACGGTCTAACAAGGCCAG-3' (R); NF-κB: 5'-ATG GCAGACGATGATCCCTAC-3' (F), 5'-CGGAAT CGAAATCCCCTCTGTT-3' (R); TNF-α: 5'-CTACCT TGTTGCCTCCTCTTT-3' (F), 5'-CGATCACCCCGA AGTTCAGTAG-3' (R); IL-1: 5'-AGTATCAGCAAC GTCAAGCAA-3' (F), 5'-TCCAGATCATGGGTTATG GACTG-3' (R). The relative expressions of mRNAs were calculated and quantified using the $2^{-\Delta\Delta CT}$ method.

ELISA assay

Mouse IL-6 Uncoated ELISA Kit and Mouse IFN-γ Uncoated ELISA Kit obtained from Invitrogen (Carlsbad, CA, USA) were used as per the manufactures instructions to quantify soluble IL-6 and IFN-γ expression of mouse serum. Optical density (OD) was blanked and measured at 450 nm.

Statistical analysis

SPSS software (version 24.0, SPSS Inc., Chicago, IL, USA) was used for statistical analysis. The results were presented as mean ± SEM and subjected to the Two-way ANOVA followed by the Student's *t*-tests, $P < 0.05$ indicates significant difference. Principal coordinate analysis, alpha diversity, beta diversity, and KEGG enrichment analysis were performed to analyze the sequencing results of mouse gut microbiota.

Results

Induction of T2DM and ameliorated effects of LDR

After 12-weeks feeding with HFD, the weight of mice increased obviously compared with control group, until

16 weeks, weight increased slowly (Fig. 1a). The results of glucose tolerance test showed that the blood glucose of HFD-fed mice reached the maximum level at 30 min after intraperitoneal injection, and the glucose levels were significantly higher than control group (Fig. 1b). In order to establish a typical T2DM mice model, STZ was intraperitoneally injected to the HFD-fed mice. The results in Fig. 1c shown that the blood sugar value reached for 11.66 ± 0.86 mmol/L in T2DM group, indicating the successful establishment of T2DM model. Subsequently, T2DM mice were exposed to the LDR according to the workflow shown in Fig. 1d. LDR intervention significantly reduced blood glucose level compared with T2DM group (Fig. 1e). HE staining results showed that islet architecture was complete in control group, which was with clear boundary, and the β cell nucleus was round, but the islet structure was damage seriously in T2DM mice, islets of T2DM mice were accompanied with scattered inflammatory cell aggregation. LDR intervention displayed a markedly protective effect on the size and structure of the islets (Fig. 1f). Meanwhile, the body weight decreased in T2DM mice after LDR exposure (Fig. 1g). These results suggest that LDR intervention can alleviate the severity of T2DM.

LDR ameliorates gut microbiota dysbiosis induced by T2DM

To study the effects of LDR on gut microbiota composition in T2DM mice, 16s rDNA sequencing was performed to evaluate and analyze the relative changes. Venn diagram showed the core microbiome in the different groups comparing the unique/shared OTUs in the gut microbiota of the mice, the number of species was 287, 208, 308 and 215 in the Con, LDR, T2DM and LDR+T2DM group, respectively (Fig. 2a). The overlapping OTUs between T2DM and LDR+T2DM groups was 174, indicating LDR markedly changed the numbers of OTUs in the gut microbiota (Fig. 2a and Fig. S1a). The outcome of principal coordinate analysis (PCoA) showed the significant differences among these four groups (Fig. 2b). Furthermore, we measured the community richness, as shown in Fig. 2c and Fig. S1b, the top 10 differential microbiota in class level and species level had significant shifts in proportional between T2DM and LDR+T2DM groups. In particular, the abundance of Desulfovibrionia and Desulfovibrio was dramatically higher in T2DM group than that in Con groups. To further determine the difference between the T2DM and LDR+T2DM, differential analysis between groups was performed at class level, the Desulfovibrionia was significantly decreased in LDR+T2DM group compared with T2DM group (Fig. 2d). Alpha diversity was used to represent the richness of species in a community, the ACE

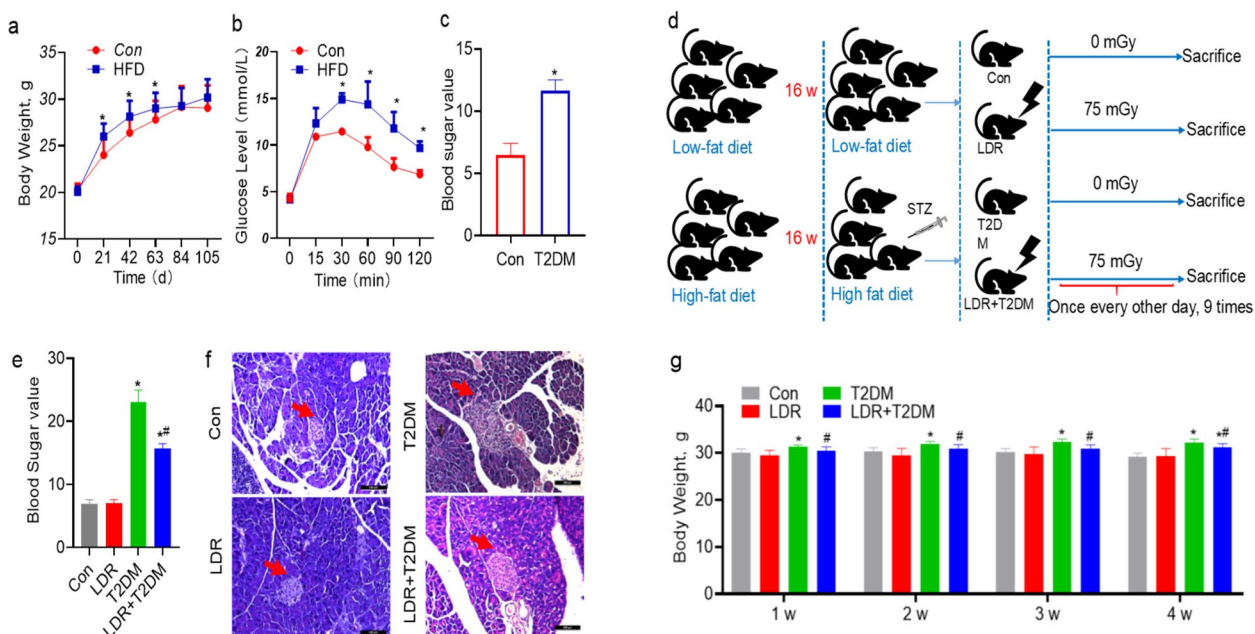


Fig. 1 LDR ameliorates impairment of HFD-induced T2DM mouse model. **a** The changes of mice body weight were measured after feeding HFD for 16 weeks, * $P < 0.05$ vs. Con. **b** The change tendency of blood glucose level in HFD-fed mice was detected by glucose tolerance test, * $P < 0.05$ vs. Con. **c** The difference of blood sugar value between Con and T2DM groups, the value was higher in T2DM group, * $P < 0.05$ vs. Con. **d** The pattern diagram of multi-LDR treatment for mice of different groups. **e** The changes of blood sugar value in mice of different groups, * $P < 0.05$ vs. Con, and # $P < 0.05$ vs. T2DM group. **f** Representative images of islets among Con, LDR, T2DM, and LDR + T2DM groups by H&E staining, scale bar = 100 μ m. **g** The body weight changes among Con, LDR, T2DM, and LDR + T2DM groups after LDR exposure, * $P < 0.05$ vs. Con; # $P < 0.05$ vs. T2DM. The results were presented as mean \pm SD

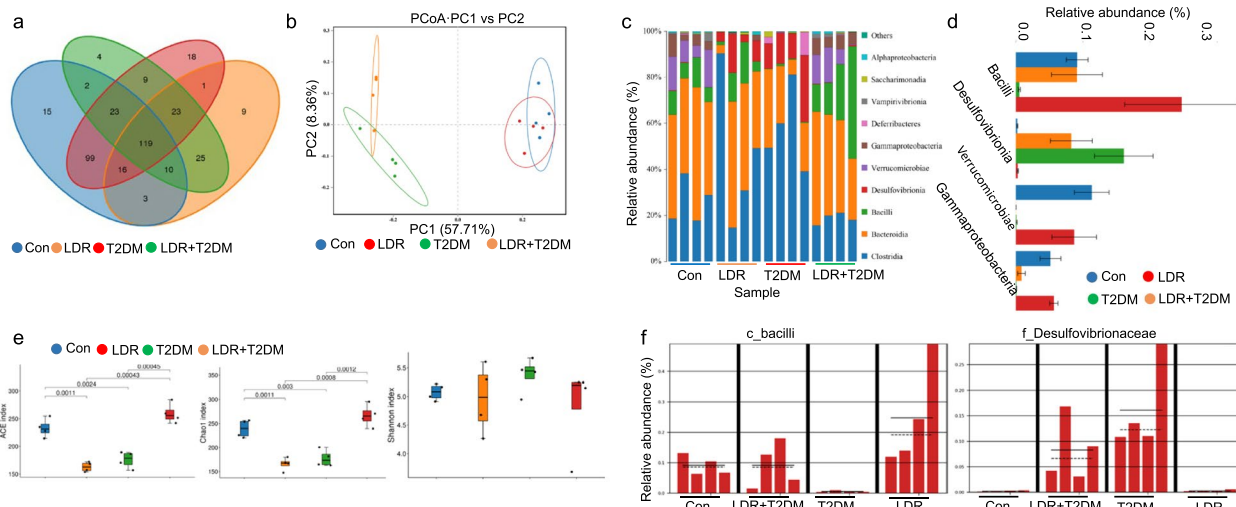


Fig. 2 LDR ameliorates gut microbiota dysbiosis induced by T2DM. **a** Venn diagram of unique/shared OTUs (operational taxonomic units) in the gut microbiota of mice from the Con, LDR, T2DM and LDR + T2DM groups, respectively. **b** The outcome of principal coordinate analysis (PCA) of the gut microbiota of mice among the four groups. The abscissa represents the first principal component, the ordinate represents the second principal component, and the percentage represents the contribution value of the principal component to the sample difference. **c** Analysis of the different communities comprising the gut microbiota at the class level among four groups. **d** The relative abundance analysis of the Bacilli, Desulfovibrionia, Verrucomicrobiae and Gammaproteobacteria at the class level among four groups. **e** Alpha-diversity indexes (ACE index, Chaos index, and Shannon index) among four groups. **f** LefSe analysis of c_bacilli and f_Desulfovibrionaceae among four groups

and Chaos index was profoundly lower in T2DM group than other groups, whereas Shannon index showed no difference (Fig. 2e). Additionally, we analyzed the relative abundance of Bacilli and Desulfovibrionaceae, the results showed that Bacilli decreased and Desulfovibrionaceae increased in T2DM group, LDR exposure could ameliorate these changes (Fig. 2f). The network diagram is a typical way to present correlation analysis, the Prevotellaceae_UCG_001 was negatively correlated with Desulfovibrio at phylum level ($P=1.474e-06$, $R^2=0.905$, Fig. S1c). KEGG pathway enrichment analysis showed that Desulfovibrionia related to 43 metabolic pathways at class level (Fig. S1d). These results suggest that LDR can ameliorate the increase of Desulfovibrionia in T2DM.

LDR altered metabolites in T2DM identified by untargeted metabolomics profiling under positive ion mode

In this study, the metabolites were measured under positive and negative ion mode, and further analyzed the correlation between metabolites and gut microbiota. As Venn graph shown in Fig. 3a, three metabolites commonly existed in four groups under positive ion mode. In addition, PCA analysis of metabolites found that the metabolites were similar in Con and LDR groups, however, there was a significantly difference in metabolic

products between T2DM and Con groups (Fig. 3b). As compared with Con group, 31 up-regulated and 45 down-regulated metabolites were screened in LDR group, while 344 up-regulated and 390 down-regulated metabolites were screened in T2DM group. Additionally, compared with T2DM group, 221 up-regulated and 176 down-regulated metabolites were screened in LDR+T2DM group (Fig. 3c and Fig. S2a). As shown in Fig. 3d and Fig. S2b, KEGG enrichment analysis found that the metabolomics mainly accumulated in mineral absorption, choline metabolism in cancer, glycerophospholipid metabolism, and ABC transporters, etc. In consistent with it, the network diagram also showed similar enrichment regularity (Fig. 3e and Fig. S2c). Compared with T2DM group, Xanthine, Kaempferol3-O-feruloyl-caffeoyl-sophoroside 7-O-glucoside, 3-Phenyl-1 H-pyrazole-4-carbaldehyde, and PE (22:1(13Z)/PGE1) significantly increased (Fig. 3f).

LDR altered metabolites in T2DM identified by untargeted metabolomics profiling under negative ion mode

Additionally, under the negative ion mode, there were 13 metabolites commonly found among Con, T2DM and LDR+T2DM groups (Fig. 4a). As shown in Fig. 4b, in T2DM and LDR+T2DM groups, KEGG enrichment analysis found that the metabolomics mainly

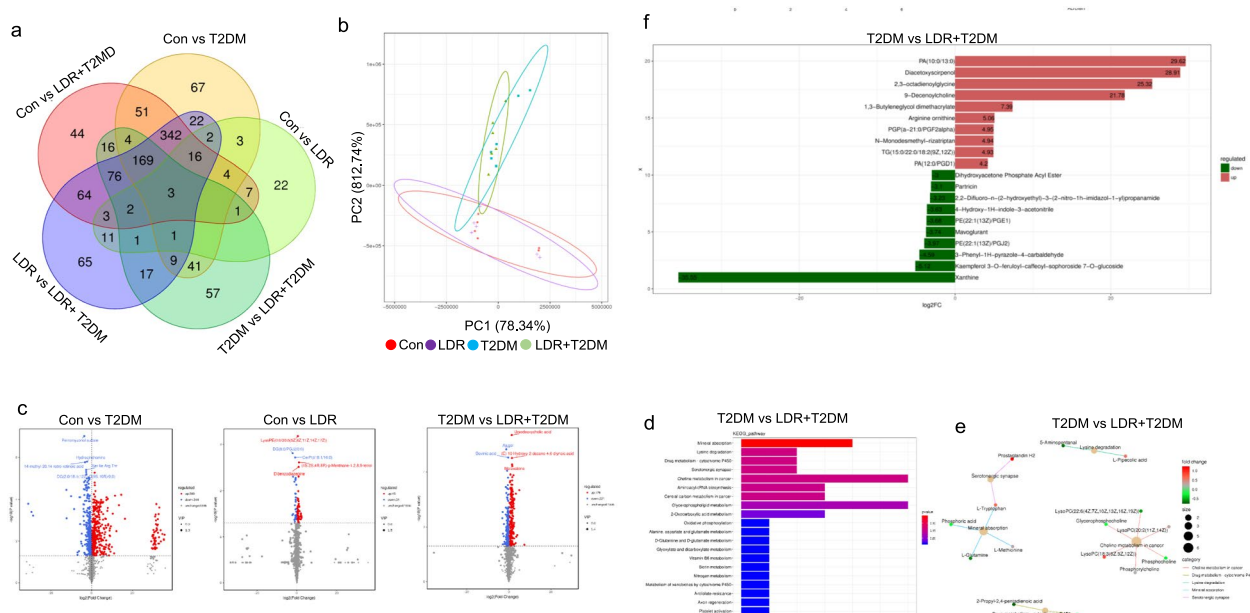


Fig. 3 LDR altered metabolites in T2DM under positive ion mode. **a** Venn diagram of differential metabolites of mouse serum from the Con, LDR, T2DM and LDR + T2DM groups, respectively. **b** The outcome of principal coordinate analysis (PCA) of the mouse serum among the four groups. The abscissa represents the first principal component, the ordinate represents the second principal component. **c** Volcano plot of metabolites from Con, LDR, T2DM and LDR + T2DM groups (The blue dots represent down-regulated metabolites, red dots represent up-regulated metabolites). **d** The enrichment analysis of differential metabolite KEGG pathway of T2DM vs. LDR + T2DM. **e** Network diagram of metabolite enrichment of T2DM vs. LDR + T2DM. **f** The differential fold analysis, the top ten metabolites in T2DM and LDR + T2DM were shown (Red bar represents up-regulation, and green bar represent down-regulation)

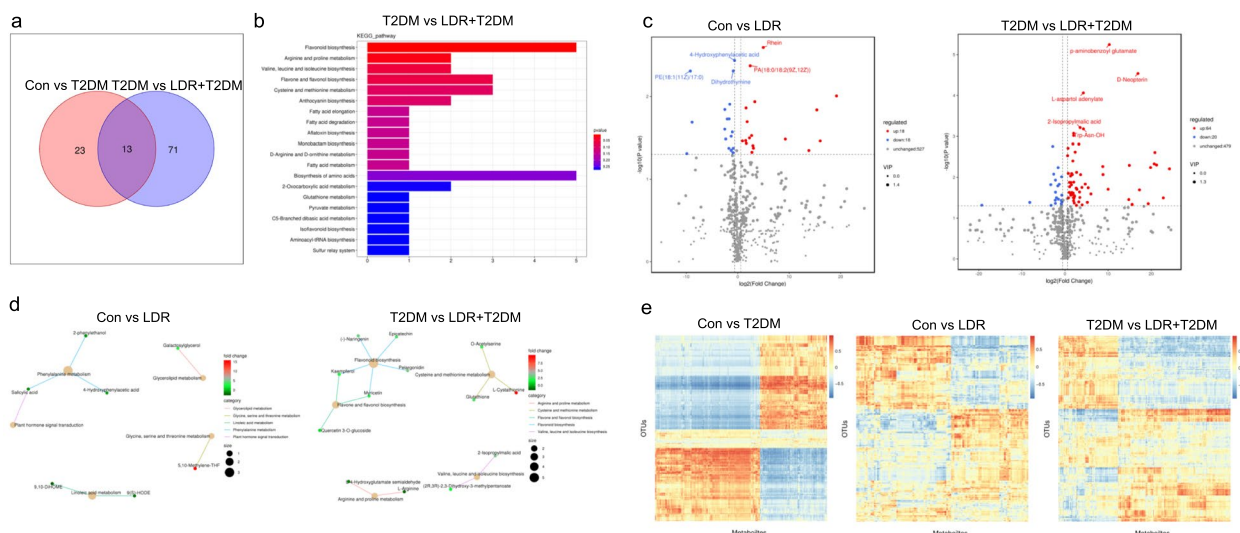


Fig. 4 LDR altered metabolites in T2DM under negative ion mode. **a** Venn diagram of differential metabolites of mouse serum from the Con, T2DM and LDR + T2DM groups, respectively. **b** The enrichment analysis of differential metabolite KEGG pathway, T2DM vs. LDR + T2DM was shown. The abscissa represents the numbers of differential metabolites, the ordinate represents the pathway. **c** Volcano plot of metabolites from four groups, Con vs. LDR and T2DM vs. LDR + T2DM was shown. Each point in volcano plot represents a metabolite, the abscissa represents the fold changes of each substance, the ordinate represents the *p*-value of the *t*-test. The blue dots represent down-regulated metabolites, red dots represent up-regulated metabolites, gray dots represent the metabolites with insignificant difference. **d** Network diagram of metabolite enrichment, the pale-yellow nodes represent pathway, and the small nodes connected to them represent the specific metabolites annotated to the pathway, Con vs. LDR and T2DM vs. LDR + T2DM was shown. **e** The correlation analysis between differential metabolites in serum and OTUs in gut microbiota of mice from the Con, LDR, T2DM and LDR + T2DM groups, respectively. The abscissa represents the metabolites, the ordinate represents the OTUs

accumulated in flavonoid biosynthesis, biosynthesis of amino acids, flavone and flavonol biosynthesis, cysteine and methionine metabolism, etc. Compared with Con group, 18 up-regulated and 18 down-regulated metabolites were screened in T2DM group. Compared with T2DM group, 64 up-regulated and 20 down-regulated metabolites were screened in LDR+T2DM group (Fig. 4c). As shown in Fig. 4d, the network diagram showed the similar enrichment regularity. As shown in Fig. 4e, combined analysis of microbiota and metabolomics found that OTUs in the gut microbiota were associated with metabolites.

The inflammation was alleviated by LDR through inhibiting TLR4/MyD88/NF-κB pathway in T2DM

IL-4 and IL-17 A expression in spleen cells were detected by Flow Cytometry, as shown in Fig. 5a and b, IL-4 positive cells were significantly decreased, while IL-17 A positive cells were significantly increased in T2DM group (*P*<0.05). However, these changes were alleviated in LDR + T2DM group, suggesting that LDR could activate the immune response. Furthermore, we measured the expressions of TLR4, MyD88, p-NF-κB p65 and p-p38 in intestine tissue through IHC. Compared with Con, these protein expressions increased in T2DM group, while they decreased in LDR + T2DM group, suggesting the

activation of TLR4/MyD88/NF-κB pathway in T2DM, which was inhibited by LDR (Fig. 5c). In line with it, the qRT-PCR results showed the mRNA expressions of TNF-α and IL-1 increased in T2DM group but decreased in LDR + T2DM group (Fig. 5d). The expression of IL-6 and IFN-γ in serum increased in T2DM group but decreased in LDR + T2DM group according to ELISA results (Fig. 5e).

Conclusion

These results suggest that LDR may exert a beneficial role in T2DM by modulating gut microbiota and metabolites, especially in TLR4/MyD88/NF-κB signaling pathway.

Discussion

Recent studies have highlighted the pivotal role of the LDR in diabetes mellitus [31, 32]. Clinical cases showed that the patient’s condition improved, and high glucose levels reduced to normal level following radon therapy, which indicated the potential improvement of type 1 diabetes treated by LDR [33]. Additionally, several reports described the mitigation of diabetes following LDR exposure, for instance, Tsuruga et al. showed that LDR (γ-rays) exposure to diabetic mice resulted in the improved glucose clearance and attenuation in pancreatic islet degeneration [32]. Guo et al. found that repeated LDR (75 mGy

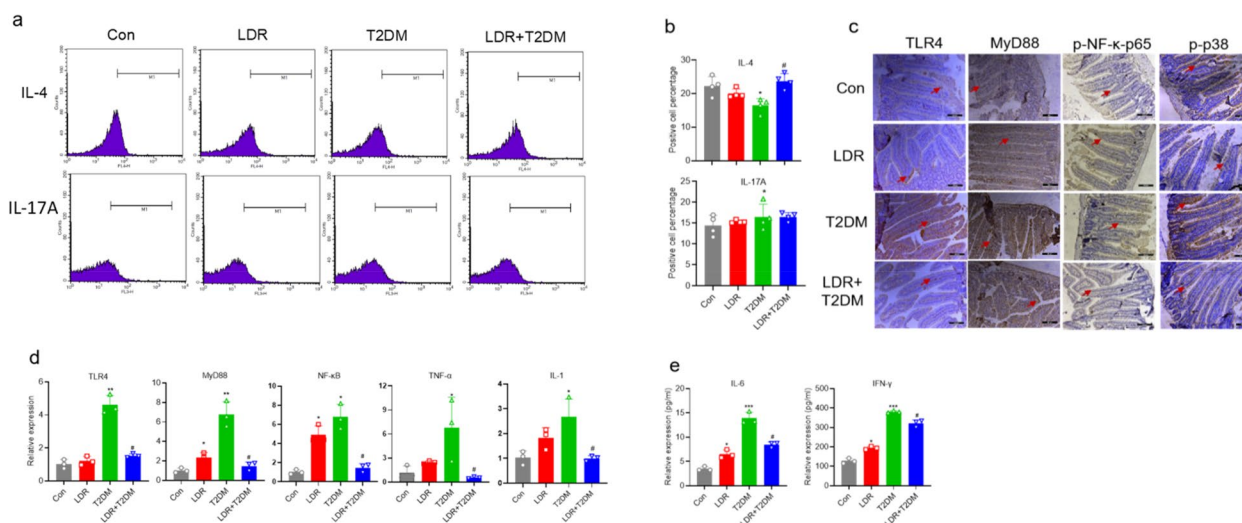


Fig. 5 LDR alleviated the inflammation of T2DM mice through inhibiting TLR4/MyD88/NF-κB pathway. **a** Representative flow cytometry images of positive cells expressed IL-4 and IL-17 A in spleen cells from Con, LDR, T2DM, and LDR+T2DM groups. **b** The percentage of positive cells expressed IL-4 and IL-17 A in spleen cells from Con, LDR, T2DM, and LDR+T2DM groups. **c** The expressions of TLR4, MyD88, p-NF-κB-p56, and p-p38 protein in mouse intestine by IHC in Con, LDR, T2DM, and LDR+T2DM groups, scale bar = 100 μm. **d** The expression of TLR4, MyD88, NF-κB, TNF-α, and IL-1 mRNA in mouse intestine analyzed by qRT-PCR. **e** The expression of IL-6 and IFN-γ in mouse serum analyzed by ELISA. Results were presented as mean ± SD, **P* < 0.05, ***P* < 0.01, ****P* < 0.001 vs. Con; #*P* < 0.05 vs. T2DM

X-ray) treated diabetic animals showed quicker skin wound healing [34]. Animal models and clinical observations suggest that LDR can alleviate diabetes; however, the mechanism is the subject of further investigation. In this study, we found that repeated LDR (75 mGy of X-ray, dose rate=0.0134 Gy/min) exposure to the type 2 diabetes mellitus (T2DM) mice induced by high-fat diet and STZ can decrease the glucose level, which is similar to previous reports.

The gut microbiota is a complex ecosystem made up of a community of microorganisms, the primary characteristics of the gut microbiota dysbiosis is the decreased diversity and abundance [35]. This can lead to the emergence of obesity, metabolic disorders, and T2DM [36, 37]. The patients with T2DM would also have some alterations of the gut microbiota, including the decreased Lactobacillus, Clostridium, and Bifidobacterium genera, while the increased Escherichia coli, Enterococcus, Bacteroidetes, and Desulfovibrio [12, 13]. In this study, the bacterial diversity of the gut microbiota in T2DM group displayed the similar changes. The increased Desulfovibrionia in T2DM group indicated that it played harmful effect in the generation and development of T2DM. However, for T2DM mice exposed to LDR, the diversity changes of Bacilli and Desulfobacterota were ameliorated, which indicated that LDR could increase the beneficial bacteria and inhibit the harmful bacteria. Some studies consistently showed that the Proteobacteria, Verrucomicrobia, Alistipes, and Akkermancia were relatively more abundant after ionizing radiation exposure, whereas

Bacteroidetes, Firmicutes, and Lactobacillus were relatively reduced [38–40]. Thus, it would be useful to develop a strategy for modifying gut microbiota to prevent T2DM.

Additionally, gut microbiota and its metabolites might involve in the process of T2DM. Studies have indicated that patients with T2DM are often associated with intestinal flora disorders and dysfunction, and the metabolites of gut microbiota, such as bile acids (BAs), short-chain fatty acids (SCFAs) and amino acids, may result in insulin sensitivity and regulate the immune homeostasis [41]. In this study, we found that metabolites detected in the blood of T2DM mice induced by HFD were obviously different. These differences include the mineral absorption, choline metabolism in cancer, glycerophospholipid metabolism and ABC transporters, flavonoid biosynthesis, biosynthesis of amino acids, flavone and flavonol biosynthesis, cysteine and methionine metabolism, etc. T2DM is one of the most common metabolic disorders. Gut microbiota can modulate the gut barrier integrity and human metabolism to take part in the synthesis of metabolites. Nevertheless, LDR may play roles in improving the metabolic patterns of T2DM, thereby easing the damage of diabetes (inflammation and insulin resistance, etc.). To investigate how LDR ameliorates the impairment of T2DM, we analyzed the relationships between gut microbiota and metabolites, and the results showed that LDR could increase the abundance of Bacilli, and decrease the abundance

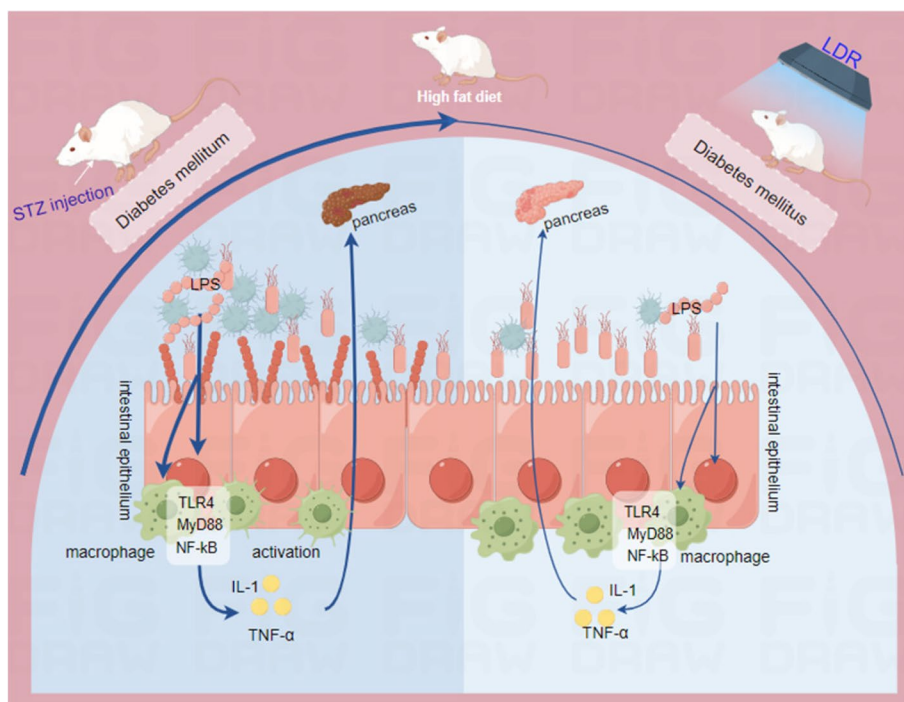


Fig. 6 Schematic model of LDR protected HFD-induced T2DM. Mice were feeding with HFD for 16 weeks and injected STZ for 5 days to induce T2DM. Desulfovibrionaceae was increased in T2DM group mice and the TLR4/MyD88/NF- κ B pathway was activated to mediate the inflammation, which might be impaired by the LDR

of Desulfovibrionaceae to produce crucial metabolites, including SCFAs, LPS, and amino acids. LPS is the main product of Desulfovibrio, and it can induce inflammation and insulin resistance through TLRs signaling pathway [19]. In this study, we found that HFD-induced T2DM mice model has increased Desulfovibrionia and activate the TLR4/MyD88/NF- κ B pathway, furthermore, TNF- α and IL-1 increased in intestine. In addition, the percentage of anti-inflammatory factor IL-4⁺ cells decreased, while the percentage of proinflammatory factor IL-17 A⁺ cells increased in T2DM group in spleen, and these changes were ameliorated by LDR. According literature, LDR can trigger immune system excitatory effects and inflammation is a basic immunological effector process in response to harmful stimuli [42]. 0.3~0.7 Gy was among the dose range of the mechanisms reported to contribute to an anti-inflammatory effects of intermediate dose exposure [43–45]. These data indicate that the activation of the immune system excitatory effects and anti-inflammation effect of LDR may be the mechanisms of LDR ameliorating T2DM impairment.

However, several relative topics about mechanisms still need to explore. Linear no-threshold (LNT) model of ionizing radiation assumes that even very low doses radiation has adverse effects on human health, but another voice demonstrates that the unique biological

effect caused by LDR is beneficial [46, 47]. Previous studies have showed that LDR played the protective roles in diabetic impairments [22–24]; however, there were different voice against the protection [48]. Actually, we used lower exposure doses and dose rates (0.0134 Gy/min), and there were 48 h for damage repair, which may be the possible reasons for difference among experiments. In this study, in T2DM mice, we found the gut microbiota disrupted, especially with an increase in Desulfovibrionia, activating of TLR4/MyD88/NF- κ B pathways and inflammatory reaction. LDR can partially correct the microbiota disruption and alleviate inflammation, the TLR4/MyD88/NF- κ B pathway may play an important role in this process, but the upstream molecules that trigger this pathway need further exploration, especially the changes in metabolic products of Desulfovibrionia have not been accurately measured. Even, fecal microbiota transplantation (FMT) of Desulfovibrionia might provide a more detailed molecular mechanism of protective effects on T2DM. Based on the results described above, we have demonstrated a potential role of LDR in protecting HFD-induced T2DM from processing through gut microbiota and metabolism. Especially, Desulfovibrio increased and the TLR4/MyD88/NF- κ B pathway was activated to mediate the inflammation, which might be impaired by the LDR (Fig. 6).

Supplementary Information

The online version contains supplementary material available at <https://doi.org/10.1186/s12902-025-01861-z>.

Supplementary Material 1.

Acknowledgements

Thank you to all the authors for their joint efforts in successfully completing the article.

Clinical trial number

Not applicable.

Authors' contributions

Conception, design, writing review and editing: Zhicheng Wang, Huan He. Design, investigation, validation, writing original draft: Lijing Qin, Rongrong Liu. Data curation, supervision, investigation: Zhen Jia, Weiqiang Xu. Resources, data curation: Li Wang, Hongyuan Tian. Software: Xinru Lian Wen Li, Yali Qi. All authors have read and agreed to the published version of the manuscript.

Funding

This work was supported by the Science and Technology Development Plan of Jilin (20240101275JC, YDZJ202201ZYTS153 and YDZJ202401200ZYTS).

Data availability

The data and materials presented in this study are available on request from the corresponding author. The datasets generated and analyzed during the current study are available in the Sequence Read Archive (SRA) repository, PRJNA1210971.

Declarations

Ethics approval and consent to participate

The animal experiments in this study were approved after strict review by the Ethics Review Committee of the School of Public Health, Jilin University, Approval No. is 2024-07-004.

Consent for publication

Not applicable.

Competing interests

The authors declare no competing interests.

Author details

¹NHC Key Laboratory of Radiobiology, School of Public Health, Jilin University, Changchun, Jilin 130021, People's Republic of China. ²Department of Oncology, The First Hospital of Hebei Medical University, Shijiazhuang, Hebei 050000, People's Republic of China. ³Jilin Medical University, Jilin, Jilin 132013, People's Republic of China.

Received: 19 September 2024 Accepted: 31 January 2025

Published online: 07 February 2025

References

- Holman N, Young B, Gadsby R. Current prevalence of type 1 and type 2 diabetes in adults and children in the UK. *Diabet Med*. 2015;32:1119–20. <https://doi.org/10.1111/dme.12791>.
- Bruno G, Runzo C, Cavallo-Perin P, Merletti F, Rivetti M, Pinach S, Novelli G, Trovati M, Cerutti F, Pagano G. Incidence of type 1 and type 2 diabetes in adults aged 30–49 years: the population-based registry in the province of Turin, Italy. *Diabetes Care*. 2005;28:2613–9. <https://doi.org/10.2337/diaca-re.28.11.2613>.
- Lee SH, Park SY, Choi CS. Insulin resistance: from mechanisms to therapeutic strategies. *Diabetes Metabolism J*. 2022;46:15–37. <https://doi.org/10.4093/dmj.2021.0280>.
- Salgado MK, Oliveira LGS, Costa GN, Bianchi F, Sivieri K. Relationship between gut microbiota, probiotics, and type 2 diabetes mellitus. *Appl Microbiol Biotechnol*. 2019;103:9229–38. <https://doi.org/10.1007/s00253-019-10156-y>.
- Heine RJ, Diamant M, Mbanya JC, Nathan DM. Management of hyperglycaemia in type 2 diabetes: the end of recurrent failure? *BMJ (Clinical Res ed)*. 2006;333:1200–4. <https://doi.org/10.1136/bmj.39022.462546.80>.
- Ahmed Y, Ali ZY, Mohamed MA, Rashed LA, Mohamed EK. Impact of combined therapy of mesenchymal stem cells and sitagliptin on a metabolic syndrome rat model. *J Diabetes Metab Disord*. 2021;20:551–60. <https://doi.org/10.1007/s40200-021-00778-3>.
- Dugas LR, Lie L, Plange-Rhule J, Bedu-Addo K, Bovet P, Lambert EV, Forrester TE, Luke A, Gilbert JA, Layden BT. Gut microbiota, short chain fatty acids, and obesity across the epidemiologic transition: the METS-Microbiome study protocol. *BMC Public Health*. 2018;18:18. <https://doi.org/10.1186/s12889-018-5879-6>.
- Conteh AR, Huang R. Targeting the gut microbiota by Asian and western dietary constituents: a new avenue for diabetes. *Toxicol Res*. 2020;9:569–77. <https://doi.org/10.1093/toxres/tfaa065>.
- Zhu B, Wang X, Li L. Human gut microbiome: the second genome of human body. *Protein Cell*. 2010;1:718–25. <https://doi.org/10.1007/s13238-010-0093-z>.
- Bäckhed F, Ding H, Wang T, Hooper LV, Koh GY, Nagy A, Semenkovich CF, Gordon JI. The gut microbiota as an environmental factor that regulates fat storage. *Proc Natl Acad Sci USA*. 2004;101:15718–23. <https://doi.org/10.1073/pnas.0407076101>.
- Le Chatelier E, Nielsen T, Qin J, Prifti E, Hildebrand F, Falony G, Almeida M, Arumugam M, Batto JM, Kennedy S, et al. Richness of human gut microbiome correlates with metabolic markers. *Nature*. 2013;500:541–6. <https://doi.org/10.1038/nature12506>.
- Wu X, Ma C, Han L, Nawaz M, Gao F, Zhang X, Yu P, Zhao C, Li L, Zhou A, et al. Molecular characterisation of the faecal microbiota in patients with type II diabetes. *Curr Microbiol*. 2010;61:69–78. <https://doi.org/10.1007/s00284-010-9582-9>.
- Lê KA, Li Y, Xu X, Yang W, Liu T, Zhao X, Tang YG, Cai D, Go VL, Pandol S, et al. Alterations in fecal *Lactobacillus* and *Bifidobacterium* species in type 2 diabetic patients in Southern China population. *Front Physiol*. 2012;3. <https://doi.org/10.3389/fphys.2012.00496>.
- Cani PD, Possemiers S, Van de Wiele T, Guiot Y, Everard A, Rottier O, Geurts L, Naslain D, Neyrinck A, Lambert DM, et al. Changes in gut microbiota control inflammation in obese mice through a mechanism involving GLP-2-driven improvement of gut permeability. *Gut*. 2009;58:1091–103. <https://doi.org/10.1136/gut.2008.165886>.
- Donath MY, Dinarello CA, Mandrup-Poulsen T. Targeting innate immune mediators in type 1 and type 2 diabetes. *Nat Rev Immunol*. 2019;19:734–46. <https://doi.org/10.1038/s41577-019-0213-9>.
- Maier HJ, Schips TG, Wietelmann A, Krüger M, Brunner C, Sauter M, Klingel K, Böttger T, Braun T, Wirth T. Cardiomyocyte-specific IκB kinase (IKK)/NF-κB activation induces reversible inflammatory cardiomyopathy and heart failure. *Proc Natl Acad Sci USA*. 2012;109:11794–9. <https://doi.org/10.1073/pnas.1116584109>.
- Góralczyk-Birńkowska A, Szmajda-Krygier D, Kozłowska E. The Microbiota-Gut-Brain Axis in Psychiatric disorders. *Int J Mol Sci*. 2022;23:23. <https://doi.org/10.3390/ijms231911245>.
- Cani PD, Bibiloni R, Knauf C, Waget A, Neyrinck AM, Delzenne NM, Burcelin R. Changes in gut microbiota control metabolic endotoxemia-induced inflammation in high-fat diet-induced obesity and diabetes in mice. *Diabetes*. 2008;57:1470–81. <https://doi.org/10.2337/db07-1403>.
- Ma Q, Li Y, Li P, Wang M, Wang J, Tang Z, Wang T, Luo L, Wang C, Wang T, et al. Research progress in the relationship between type 2 diabetes mellitus and intestinal flora. *Biomed Pharmacotherapy = Biomedicine Pharmacotherapie*. 2019;117:117. <https://doi.org/10.1016/j.biopha.2019.109138>.
- Palacios T, Vitetta L, Coulson S, Madigan CD, Lam YY, Manuel R, Briskey D, Hendy C, Kim JN, Ishoey T, et al. Targeting the intestinal microbiota to prevent type 2 diabetes and enhance the Effect of Metformin on Glycaemia: a Randomised Controlled Pilot Study. *Nutrients*. 2020;12. <https://doi.org/10.3390/nu12072041>.
- Kataoka T. Study of antioxidative effects and anti-inflammatory effects in mice due to low-dose X-irradiation or radon inhalation. *J Radiat Res*. 2013;54:587–96. <https://doi.org/10.1093/jrr/rs1141>.

22. Zhang C, Tan Y, Guo W, Li C, Ji S, Li X, Cai L. Attenuation of diabetes-induced renal dysfunction by multiple exposures to low-dose radiation is associated with the suppression of systemic and renal inflammation. *Am J Physiol Endocrinol Metab.* 2009;297:E1366–1377. <https://doi.org/10.1152/ajpendo.00478.2009>.
23. Zhang C, Jin S, Guo W, Li C, Li X, Rane MJ, Wang G, Cai L. Attenuation of diabetes-induced cardiac inflammation and pathological remodeling by low-dose radiation. *Radiat Res.* 2011;175:307–21. <https://doi.org/10.1667/rr1950.1>.
24. Zhao H, Xu S, Wang Z, Li Y, Guo W, Lin C, Gong S, Li C, Wang G, Cai L. Repetitive exposures to low-dose X-rays attenuate testicular apoptotic cell death in streptozotocin-induced diabetes rats. *Toxicol Lett.* 2010;192:356–64. <https://doi.org/10.1016/j.toxlet.2009.11.011>.
25. Liu X, Zhou Y, Wang S, Guan H, Hu S, Huang R, Zhou P. Impact of low-dose ionizing radiation on the composition of the gut microbiota of mice. *Toxicol Sci.* 2019;171:258–68. <https://doi.org/10.1093/toxsci/kfz144>.
26. Caesar R, Reigstad CS, Bäckhed HK, Reinhardt C, Ketonen M, Lundén G, Cani PD, Bäckhed F. Gut-derived lipopolysaccharide augments adipose macrophage accumulation but is not essential for impaired glucose or insulin tolerance in mice. *Gut.* 2012;61:1701–7. <https://doi.org/10.1136/gutjnl-2011-301689>.
27. Erridge C, Attina T, Spickett CM, Webb DJ. A high-fat meal induces low-grade endotoxemia: evidence of a novel mechanism of postprandial inflammation. *Am J Clin Nutr.* 2007;86:1286–92. <https://doi.org/10.1093/ajcn/86.5.1286>.
28. Xiao S, Fei N, Pang X, Shen J, Wang L, Zhang B, Zhang M, Zhang X, Zhang C, Li M, et al. A gut microbiota-targeted dietary intervention for amelioration of chronic inflammation underlying metabolic syndrome. *FEMS Microbiol Ecol.* 2014;87:357–67. <https://doi.org/10.1111/1574-6941.12228>.
29. Zhang-Sun W, Augusto LA, Zhao L, Caroff M. *Desulfovibrio desulfuricans* isolates from the gut of a single individual: structural and biological lipid a characterization. *FEBS Lett.* 2015;589:165–71. <https://doi.org/10.1016/j.febslet.2014.11.042>.
30. Franko A, von Kleist-Retzow JC, Neschen S, Wu M, Schommers P, Böse M, Kunze A, Hartmann U, Sanchez-Lasheras C, Stoehr O, et al. Liver adapts mitochondrial function to insulin resistant and diabetic states in mice. *J Hepatol.* 2014;60:816–23. <https://doi.org/10.1016/j.jhep.2013.11.020>.
31. Zhang C, Xing X, Zhang F, Shao M, Jin S, Yang H, Wang G, Cui J, Cai L, Li W, et al. Low-dose radiation induces renal SOD1 expression and activity in type 1 diabetic mice. *Int J Radiat Biol.* 2014;90:224–30. <https://doi.org/10.3109/09553002.2014.877174>.
32. Tsuruga M, Taki K, Ishii G, Sasaki Y, Furukawa C, Sugihara T, Nomura T, Ochiai A, Magae J. Amelioration of type II diabetes in db/db mice by continuous low-dose-rate gamma irradiation. *Radiat Res.* 2007;167:592–9. <https://doi.org/10.1667/rr0786.1>.
33. Kojima S, Cuttler JM, Shimura N, Koga H, Murata A, Kawashima A. Radon Therapy for Autoimmune diseases Pemphigus and Diabetes: 2 case reports. Dose-response: Publication Int Hormesis Soc. 2019;17:1559325819850984. <https://doi.org/10.1177/1559325819850984>.
34. Guo WY, Wang GJ, Wang P, Chen Q, Tan Y, Cai L. Acceleration of diabetic wound healing by low-dose radiation is associated with peripheral mobilization of bone marrow stem cells. *Radiat Res.* 2010;174:467–79. <https://doi.org/10.1667/rr1980.1>.
35. Shin NR, Whon TW, Bae JW. Proteobacteria: microbial signature of dysbiosis in gut microbiota. *Trends Biotechnol.* 2015;33:496–503. <https://doi.org/10.1016/j.tibtech.2015.06.011>.
36. Kowalewska B, Zorena K, Szmigiero-Kawko M, Wąż P, Myśliwiec M. Higher diversity in fungal species discriminates children with type 1 diabetes mellitus from healthy control. *Patient Prefer Adherence.* 2016;10:591–9. <https://doi.org/10.2147/ppa.S97852>.
37. Marchesi JR, Adams DH, Fava F, Hermes GD, Hirschfield GM, Hold G, Quraishi MN, Kinross J, Smidt H, Tuohy KM, et al. The gut microbiota and host health: a new clinical frontier. *Gut.* 2016;65:330–9. <https://doi.org/10.1136/gutjnl-2015-309990>.
38. Fernandes A, Oliveira A, Soares R, Barata P. The effects of Ionizing Radiation on Gut Microbiota: what can Animal models tell us?—A systematic review. *Curr Issues Mol Biol.* 2023;45:3877–910. <https://doi.org/10.3390/cimb45050249>.
39. Yu Y, Lin X, Feng F, Wei Y, Wei S, Gong Y, Guo C, Wang Q, Shuai P, Wang T, et al. Gut microbiota and ionizing radiation-induced damage: is there a link? *Environ Res.* 2023;229:115947. <https://doi.org/10.1016/j.envres.2023.115947>.
40. Zhang S, Wang Q, Zhou C, Chen K, Chang H, Xiao W, Gao Y. Colorectal cancer, radiotherapy and gut microbiota. *Chin J cancer Res = Chung-kuo Yen Cheng Yen Chiu.* 2019;31:212–22. <https://doi.org/10.21147/j.jssn.1000-9604.2019.01.16>.
41. Liu L, Zhang J, Cheng Y, Zhu M, Xiao Z, Ruan G, Wei Y. Gut microbiota: a new target for T2DM prevention and treatment. *Front Endocrinol.* 2022;13:958218. <https://doi.org/10.3389/fendo.2022.958218>.
42. Lumniczky K, Impens N, Armengol G, Candéas S, Georgakilas AG, Hornhardt S, Martin OA, Rödel F, Schaeue D. Low dose ionizing radiation effects on the immune system. *Environ Int.* 2021;149:106212. <https://doi.org/10.1016/j.envint.2020.106212>.
43. Roedel F, Kley N, Beuscher HU, Hildebrandt G, Keilholz L, Kern P, Voll R, Herrmann M, Sauer R. Anti-inflammatory effect of low-dose X-irradiation and the involvement of a TGF-beta1-induced down-regulation of leukocyte/endothelial cell adhesion. *Int J Radiat Biol.* 2002;78:711–9. <https://doi.org/10.1080/09553000210137671>.
44. Kern PM, Keilholz L, Forster C, Hallmann R, Herrmann M, Seegenschmiedt MH. Low-dose radiotherapy selectively reduces adhesion of peripheral blood mononuclear cells to endothelium in vitro. *Radiotherapy Oncology: J Eur Soc Therapeutic Radiol Oncol.* 2000;54:273–82. [https://doi.org/10.1016/s0167-8140\(00\)00141-9](https://doi.org/10.1016/s0167-8140(00)00141-9).
45. Hildebrandt G, Maggiorella L, Rödel F, Rödel V, Willis D, Trott KR. Mononuclear cell adhesion and cell adhesion molecule liberation after X-irradiation of activated endothelial cells in vitro. *Int J Radiat Biol.* 2002;78:315–25. <https://doi.org/10.1080/09553000110106027>.
46. Kino K. The prospective mathematical idea satisfying both radiation hormesis under low radiation doses and linear non-threshold theory under high radiation doses. *Genes Environment: Official J Japanese Environ Mutagen Soc.* 2020;42(4). <https://doi.org/10.1186/s41021-020-0145-4>.
47. Dobrzyński L, Fornalski KW, Feinendegen LE. Cancer Mortality among people living in Areas with various levels of natural background Radiation. Dose-Response. 2015;13:1559325815592391. <https://doi.org/10.1177/1559325815592391>.
48. Ju Z, Guo P, Xiang J, Lei R, Ren G, Zhou M, Yang X, Zhou P, Huang R. Low-dose radiation exaggerates HFD-induced metabolic dysfunction by gut microbiota through PA-PYCR1 axis. *Commun Biol.* 2022;5:945. <https://doi.org/10.1038/s42003-022-03929-1>.

Publisher's Note

Springer Nature remains neutral with regard to jurisdictional claims in published maps and institutional affiliations.